Dynamics of Density and Orientation Fluctuations in Supercooled Zinc Halides†

E. A. Pavlatou, S. N. Yannopoulos, and G. N. Papatheodorou*

Institute of Chemical Engineering and High Temperature Chemical Processes‡ and Department of Chemical Engineering, University of Patras, P.O. Box 1414, GR-26500 Patras, Greece

G. Fytas*

Institute of Electronic Structure and Laser,‡ P.O. Box 1527, GR-711 10 Heraklion, Crete, Greece

Received: January 28, 1997; In Final Form: May 9, 1997⊗

Photon correlation spectroscopy in both polarized and depolarized geometries has been utilized to study density and orientation fluctuations in $ZnCl_2$, $ZnBr_2$, and their symmetric mixture in the metastable supercooled state. The pure components display behavior intermediate between strong and fragile glasses reflected in the shape ($L(\log \tau)$) and dynamics (τ) of the relaxation function $C(t)$, being similar for both density ($C_\rho(t)$) and orientation ($C_2(t)$) correlation functions. In contrast to polymer blends, concentration fluctuations have no measurable broadening effect on the shape of $C(t)$. Instead, $L(\log \tau)$ becomes narrower with increasing temperature and affects differently $C_\rho(t)$ and $C_2(t)$ for the zinc halide mixture. Despite local homogeneity in the thermodynamically ideal mixture, $ZnBr_2$ with the higher glass transition temperature ($T_g = 395$ K) was found to dominate the primary α-relaxation in the symmetric binary mixture. In the framework of "two-fluid" models, the distribution and the temperature dependence of τ support rigid microheterogeneities on the order of 2 nm. The additional slow process, observed in fragile glasses so far, appears to affect also the anisotropic scattering from the pure components.

I. Introduction

Glass formation in liquids upon cooling below the melting point is a long-standing research problem[1] with implications in a wide variety of phenomena. Because of the cooperative nature of molecular motions in the metastable supercooled state, the relevant structural relaxation $C(t)$ manifests itself in different dynamic variables of the glass-forming systems. Among these, collective variables e.g. short wavelength (q^{-1}) density $\rho_q(t)$ fluctuations and reorientation dynamics are particularly useful to study glass dynamics in view of recent kinetic and thermodynamic attempts toward a theory of viscoelastic disordered materials.[2−4] The correlation function of $\rho_q(t)$ can be measured by neutron spin-echo[1c] and polarized light scattering[5] over complementary time ranges. The dynamics of the orientation fluctuations can be probed by the latter technique in the depolarized geometry[5,6] over a broad dynamic range (10^3-10^{-12} s).

Both density [$C_\rho(q,t)$] and orientation [$C_2(q,t)$] correlation functions are affected by $C(t)$, and the corresponding average relaxation times τ and τ_2 for molecular and polymeric glass formers assume, within experimental accuracy, the same value.[4,7] On the other hand, it has been recently reported[8] that translational diffusion of probe molecules in a molecular glass former displays weaker temperature (T) dependence than reorientation times near and above the calorimetric glass transition temperature T_g. These experiments, which involve center of mass motion over long distances, probably reflect a different diffusion mechanism than for the much shorter displacements probed by light scattering, where $\tau \approx \tau_2$. Besides the short-range density fluctuations which result in a q-independent $C_\rho(t)$ at low q's[9] (q being the scattering wavevector), dynamic light scattering has recently revealed[10] the presence of "long-range density fluctuations" characterized by a diffusive ($\propto q^2$) single-relaxation rate and q-dependent amplitude. In a "two-fluid" thermodynamic model[8b] these density fluctuations can be envisaged as a diffusion of heterogeneities of the dynamic (liquidlike and solidlike) states in analogy to concentration fluctuations in two-component mixtures.[11a] In this context, it should be mentioned that scattering techniques, and in particular light scattering, represent a sensitive tool to infer microheterogeneities in the supercooled state, a pertinent aspect of recent theoretical developments.[3,11]

The important features of the vitrification process can be summarized as follows: (i) nonexponential shape of $C(t)$, (ii) strong T-dependence[3,12] of the primary (α) relaxation times τ_α, (iii) bifurcation into slow (α-) and secondary (β-) relaxation,[13,14] (iv) manifestation of glass dynamics in different modes[15] in the system, (v) the presence of slow q^2-dependent process, and (vi) concentration fluctuation effects in homogeneous mixed glasses.[16] Which of these properties are universal[14] is still one of the important issues of the liquid−glass transition. The fact that the strong versus fragile classification[1b] of glass-forming systems is applicable underlines this universality distinction and moreover justifies systematic studies of different van der Waals and network glasses. Investigation of items i and ii requires experiments with a broad time range, whereas for item iv there is a need for different experimental probes.

In this paper we report photon correlation spectroscopic (PCS) experiments in amorphous $ZnCl_2$, $ZnBr_2$, and their symmetric mixture (50 mol % $ZnCl_2$). PCS has been mainly applied on amorphous polymers in order to investigate density, concentration, and optical anisotropy fluctuations near and above the glass transition temperature.[5,7] Only a few PCS studies in inorganic glasses (mixed alkali−silicate oxides,[17] $3KNO_3-2Ca(NO_3)_2$,[18] B_2O_3,[19] As_2O_3[14]) have appeared in the literature so far. Structural relaxation times of supercooled pure $ZnCl_2$ near and above T_g have not been available, although the dynamics of pure $ZnCl_2$ has been recently studied[20] by depolarized light

† Dedicated to Prof. Daniel Kivelson for his contribution to the dynamics of liquid and supercooled liquid state.

‡ Foundation for Research and Technology-Hellas (FORTH).

⊗ Abstract published in *Advance ACS Abstracts,* October 1, 1997.

S1089-5647(97)00343-X CCC: $14.00

scattering at high frequencies and hence high temperatures where mode coupling theory[2] is applicable. The relaxational characteristics of $ZnCl_2$ in the dynamic range $10^{-6}-10^3$ s, covered by PCS, are of particular interest since this network glass[1,21,22] displays intermediate behavior between strong and fragile glasses. The purpose of the present work is to investigate the density and orientation fluctuations of carefully prepared pure zinc chloride and zinc bromide and the effect of concentration fluctuations in their mixture near and above T_g, over a broad temperature range (370−700 K). To elucidate the nature of the relaxation process, we compare the obtained light scattering results with previous investigations[20,23,24] on the structural relaxation in the same system and discuss them in light of current models of the liquid−glass transition.

II. Experimental Section

Sample Preparation. The reagent grade chemicals $ZnCl_2$ and $ZnBr_2$ were purchased from Merck Chemical Co. (purity >98%) and Cerac/Pure Inc. (purity 99.5%), respectively. Since zinc halides are strongly hygroscopic, the starting materials were further purified by flowing gaseous reagents through the molten salts according to the following procedure: The chemicals were loaded in a specially designed quartz reservoir with an intervening fused silica filter of medium porosity (5−40 μm) and attached to an optical quartz tube (10 mm o.d., 8 mm i.d., and 5−6 cm length). The salts were firstly dried under vacuum by gradual heating up to 250 °C over a period of at least 4 h. Dry nitrogen was bubbled through the melt while the temperature was increased to the corresponding melting point. Nitrogen was replaced by ultrapure HCl or HBr, which was flowed through the liquid for 2−6 h. Small quantities of pure oxygen also passed through the melt for a few minutes at 600 °C, to remove traces of organic contamination. The flow of HCl or HBr continued for two more hours at 450 °C, and finally pure and dry nitrogen was passed through the melt for about 15−30 min to remove any dissolved gas. After a few hours and under low nitrogen pressure, the melt was filtered slowly into the sample tube, which was then evacuated and sealed. This procedure was applied twice to most of the samples used in this work to obtain ultrapure single salts.

All operations concerning the purified salts were carried out in a nitrogen-filled glovebox with a water content less than 1 ppm and in sealed fused silica containers. Mixtures were prepared by combining appropriate amounts of the desired zinc halides and transferring them into clean, dry, and degassed fused silica tubes (10 mm o.d., 8 mm i.d.) with a mediating quartz filter of medium porosity. The tubes containing the solid salts on the top of the filter were carefully evacuated and sealed. Afterward, they were placed in a vertical furnace at a temperature above their melting point, where the melt was filtered slowly in the lower part of the tube (optical cell), which was eventually sealed off. The pure $ZnBr_2$ was loaded in smaller optical cells (6 mm o.d., 4 mm i.d.), because zinc bromide appears to be a weaker glass former in comparison with $ZnCl_2$, consequently requiring high quenching rates and limited sample size. For making $ZnCl_2-ZnBr_2$ glasses, the cells containing the purified mixtures were heated for several hours (minimum 7 h) and then quenched in water at room temperature. All glasses were transparent, clear, free of optical defects, and dust-free. As for the majority of inorganic glass-forming molten salts, rapid crystallization occurs with increasing temperature near T_g, and thus no spectra could be obtained in the temperature range 180−250, 170−330 °C and 185−260 °C, respectively, for pure $ZnCl_2$, $ZnBr_2$, and their 50% mixture.

Photon Correlation Spectroscopy (PCS). The correlation functions $G(t)$ of the polarized light scattering intensity were mainly measured at a scattering angle of $\theta = 90°$ at different temperatures (100−420 °C). Furthermore, two additional angles (45° and 150°) were used to examine the influence of q variation on the $G(t)$ of $ZnCl_2$ and the mixture. The excitation light source was an argon ion laser (Spectra Physics 2020) operating in the single mode at 488 nm with a stabilized power of 200 mW. The incident beam was polarized vertically with respect to the scattering plane using a Glan polarizer. The scattered light from the sample was collected through a Glan-Thomson polarizer (Halle, Berlin) with an extinction coefficient better than 10^{-7}, which allowed us to detect the vertical (V) and horizontal (H) components of the scattered light and measure the corresponding correlation functions $G_{VV}(t)$ and $G_{VH}(t)$.

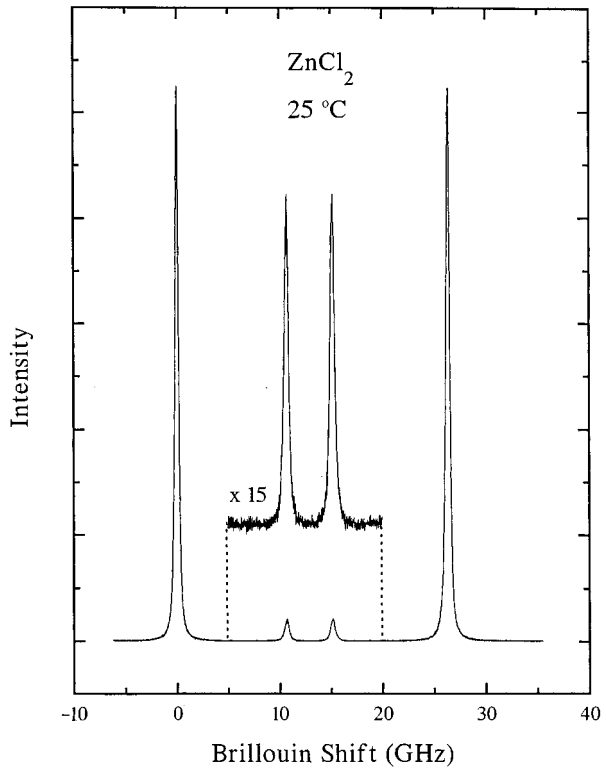

Figure 1. Polarized Rayleigh−Brillouin spectrum of $ZnCl_2$ glass.

The function $G(t)$ was measured over a nine decades in time ($10^{-6}-10^3$ s) with a full multiple tau digital correlator (ALV-5000/FAST) with 280 channels. The zinc halide samples used in this study seem to be dust-free and optically homogeneous. The samples displayed intrinsic light scattering, as indicated by the low values of the Landau−Plazcek intensity ratio in the Rayleigh−Brillouin spectra (6−8, at 25 °C); Figure 1 shows a Rayleigh−Brillouin spectrum of one of the samples at 25 °C and $\theta = 90°$ with a Landau−Plazcek ratio equal to 8. Hence, the desired normalized electric field time correlation function $g(t)$ is related to the measured $G(t)$, under the assumption of homodyne conditions, by the equation

$$G(t) = A[1 + f^*|\alpha g(t)|^2] \quad (1)$$

where A is the baseline determined at long delay times and f^* is an instrumental factor obtained from $G_{VV}(t)$ of dilute polystyrene (PS) solutions in CCl_4 ($f^* = 0.5$). The parameter α is a measure of the fraction of the total scattered intensity with correlation times longer than about 10^{-6} s.

For pure $ZnCl_2$, PCS measurements have been performed in the supercooled region from 120 to 180 °C and in the liquid state from 260 to 420 °C. The latter T range was examined to

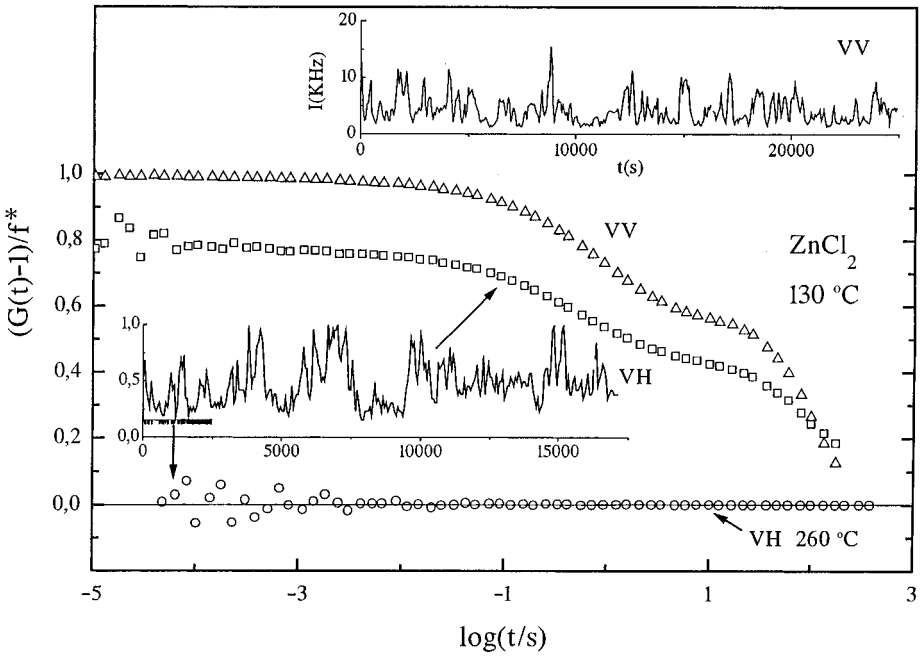

Figure 2. Polarized (VV) and depolarized (VH) intensity net correlation functions in supercooled $ZnCl_2$ at 130 °C. The depicted intensity profiles for the two scattering geometries justify the lack of baseline. Alternatively, the VH correlation function at 260 °C, far above T_g, is featureless, as anticipated from its intensity profile (inset).

verify the absence of slow dynamics in the time window of PCS. Figure 2 shows polarized and depolarized intensity net correlation $(G(t)/A - 1)/f^*$ functions at 130 and 260 °C for long accumulation times, along with the trace of the light-scattering intensities (insets); the long time fluctuations of the intensity are responsible for the slow process in both VV and VH experimental functions in the supercooled state. In the liquid state, there is no dynamic light scattering with correlation times longer than about 10^{-6} s, as demonstrated by the flat featureless $G(t)$ at 260 °C. The experimental functions of ref 25 are probably experimental artifacts. Thermal equilibrium at each measurement temperature was found to be crucial for reproducible results, but the variation of the thermal history of the sample had no measurable effect on the fast process of $G(t)$.

III. Data Analysis and Results

The scattering of light from an isotropic medium depends on the polarization of the scattered light relative to the incident beam.[26] For weak anisotropic scattering, the electric field correlation function $C_{VV}(q,t)$ of the polarized scattered light is determined by fluctuations $\delta\epsilon_{zz}(q,t)$ in the dielectric constant, which in a single-component system is proportional to the qth component of the number density fluctuation $\delta\rho(q,t) = \sum_j \exp(iqr_j(t))$, with $r_j(t)$ being the position of the jth molecule:

$$C_{VV}(q,t) \approx C_\rho(q,t) = \left(\frac{\partial\epsilon}{\partial\rho}\right)^2 \langle \delta\rho(q,t)\delta\rho^*(q,0)\rangle / \langle|\delta\rho(q,0)|^2\rangle \quad (2)$$

For $t \gg 1/uq$ with u being the adiabatic longitudinal sound velocity, $C_\rho(q,t)$ exhibits a two-step decay function due to the diffusive entropy fluctuations (heat mode) and the local order-parameter fluctuations (structural relaxation). In principle, measurement of the former by PCS requires very low q's (i.e. $\theta = 1°$) which are prone to experimental difficulties, but is straightforward by the forced Rayleigh scattering technique.[15]

The VH scattering is determined by the fluctuations of $\delta\epsilon_{yz}(q,t)$ arising from the fluctuations $\delta\alpha_{yz}(q,t) = \sum_j \alpha^j_{yz}(t) \exp(iqr_j(t))$ in the molecular optical anisotropy $\alpha_{yz}(q,t)$ of the scatterers. The correlation function $C_2(q,t)$ of the depolarized scattered light can be written in a normalized form as

$$C_2(q,t) = \langle \delta\alpha_{yz}(q,t)\delta\alpha^*_{yz}(q,0)\rangle / \langle|\delta\alpha_{yz}(q)|^2\rangle \quad (3)$$

where α^j_{yz} is the yz component of the polarizability tensor of the jth molecule. The depolarized light scattering intensity I_{VH} associated with these fluctuations is proportional to the collective optical anisotropy $\langle|\delta\alpha_{yz}(q)|^2\rangle$. The expressions entering eqs 2 and 3 in the limit $q \rightarrow 0$ relate[27] to the relaxation of longitudinal[5] and shear compliance, respectively, of mechanical experiments. In fact, for low light scattering q's, the fast process of Figure 2 was found to be insensitive to the variation of q.

The experimental correlation functions of Figure 2 exhibit two distinct decays in both VV and VH scattering. The fast process can be characterized by the function

$$g(t) = \exp[-(t/\tau^*)^\beta] \quad (4)$$

which is nonexponential for values of the shape parameter $\beta < 1$.

The relaxation function in eq 4, which does not necessarily imply temporal heterogeneities in an otherwise homogeneous system,[29] has been used in eq 1 to represent the experimental $C_{VV}(t)$ and $C_2(t)$ $(\equiv (G(t)/A - 1)/f^*)$; due to the low depolarization $(I_{VH}/I_{VV} \simeq 0.02)$ ratio, the approximation $C_{VV}(t) \simeq C_\rho(t)$ (eq 2) is justified. For $C_\rho(t)$ in $ZnCl_2$, β amounts to 0.71 $\pm$ 0.02 over the temperature range 398−450 K, one of the largest values ever observed for glass-forming liquid.[16,19,22] Figure 3 shows VV and VH correlation functions for $ZnBr_2$ and the symmetric $ZnBr_2/ZnCl_2$ mixture at $\theta = 90°$ ($q \simeq 0.025$ nm^{-1}). In contrast to the pure components, in the mixture the slow process contributes only weakly, if at all, to the dynamic anisotropic scattering. Only for $ZnCl_2$ do the experimental correlation functions (Figure 2) appear to reach baseline; that is, only for this case does the slow process relax within the time range of the PCS. The contribution of the slow process was included in the global fit of the experimental correlation functions as an exponential decay function in addition to eq 4. The orientation correlation functions $C_2(t)$ possess systematically

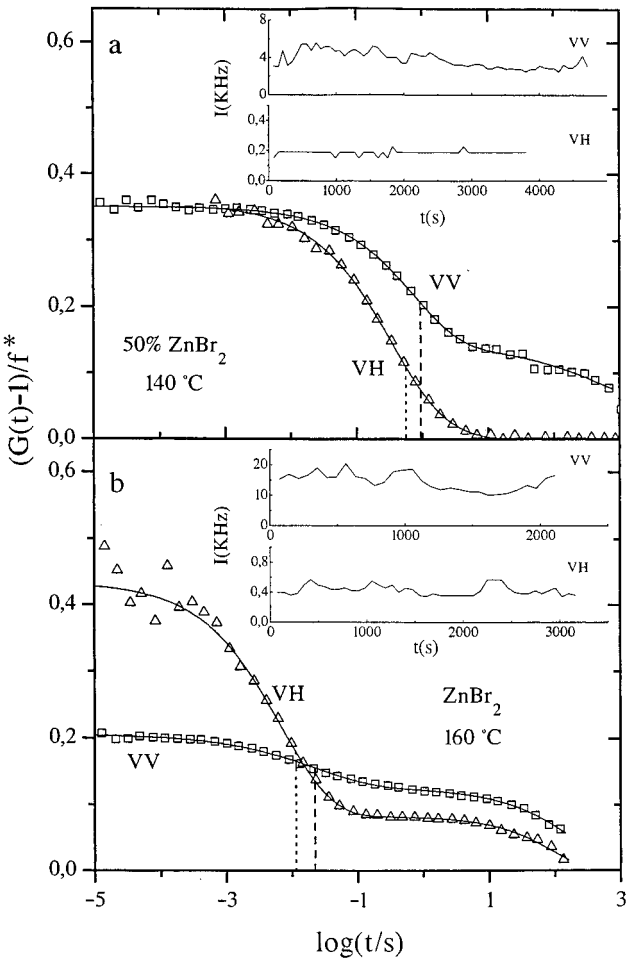

Figure 3. Polarized and depolarized intensity net correlation functions for $ZnBr_2$ and a 50% $ZnCl_2/ZnBr_2$ mixture in the supercooled state along with the traces of the total intensity shown in the insets. The vertical dashed lines indicate the relaxation time at the maximum of the distribution $L(\log \tau)$ (eq 5).

broader shape than the $C_\rho(t)$ for the pure components and the mixture; for example, for the mixture $\beta_{VH} \simeq 0.62$, $\beta_{VV} \simeq 0.72$.

An alternative fitting procedure is to employ an inverse Laplace transform (ILT) analysis with a superposition of exponentials:

$$C(t) = \int_0^\infty L(\log \tau) \exp(-t/\tau)\, \mathrm{d} \log \tau \qquad (5)$$

This equation is compatible with a microdomain (spatial heterogeneities) picture of the supercooled state.[2,11] The distributions $L(\log \tau)$ of relaxation times for the pure components and their mixture are shown in Figure 4. The width of the distribution is quite similar for the pure components and their mixture, whereas it is broader for $C_2(t)$ compared to $C_\rho(t)$. Thus, both data analyses (eqs 4 and 5) yield consistent results. The intensity $I = \alpha I^*$ associated with the fast process can be estimated from the fraction $\alpha = (\int L(\log \tau)\, \mathrm{d} \log \tau)/f^*$ and the total light-scattering intensity I^* normalized to that of the standard toluene. For both VV and VH spectral components, I is found to be insensitive to q and composition variation, and assumes the values $I_\rho = 0.5 \pm 0.1$ and $I_2 = 0.12 \pm 0.03$ relative to the VV and VH intensity of toluene, respectively; the depolarization ratio ρ_T of toluene is 0.34. Therefore, the depolarization ratio $(\rho_T I_2/I_\rho)$ for the fast process based on these intensities is about 0.1, which indicates[28] that anisotropic scattering from zinc halides should originate from fluctuations in the permanent optical anisotropy (eq 3); that is, possible

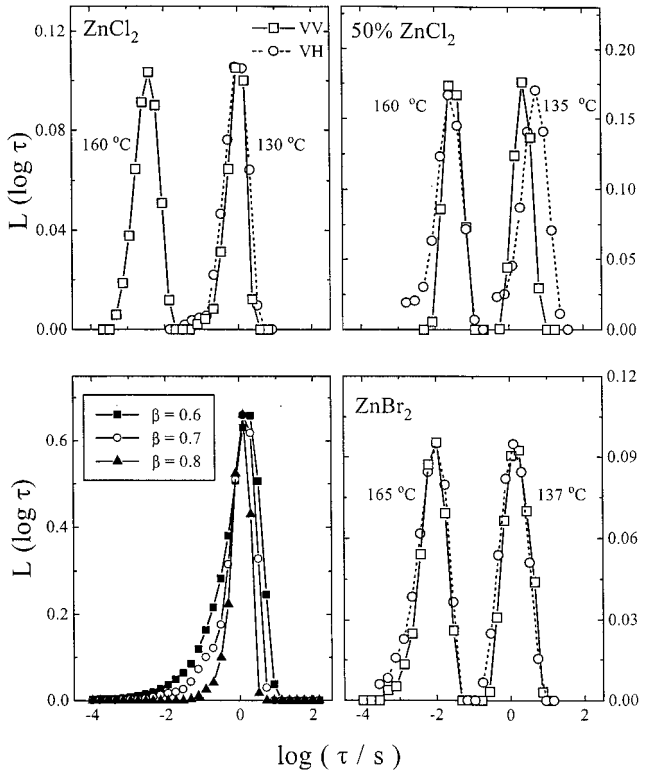

Figure 4. Distribution of relaxation times $L(\log \tau)$ (eq 5) for the fast process in the experimental polarized and depolarized time correlation functions of the pure components and their symmetric mixture. For comparison, the distribution $L(\log \tau)$ corresponding to the stretched exponential is shown (eq 4) for three values of β indicated in the plot.

contribution from slow components of interaction-induced scattering can be ignored. Further, the contribution of the VH scattering in the $I^*_{VV}(t)$ $(=I_\rho(t) + (4/3)I^*_{VH}(t))$ (eq 2) can be neglected.

IV. Discussion

Pure Components. In the coupling model of the primary α-relaxation,[29] the distribution parameter β and the temperature dependence of $\tau(T)$ near T_g are interrelated quantities. Recently, the nonexponential shape of the relaxation function obtained by different techniques and characterized by β has been correlated[22] to the non-Arrhenius dependence of $\tau(T)$. Expressing the latter in terms of fragility $m \equiv \mathrm{d} \log \tau/\mathrm{d}(T_g/T)$ at T_g, this broad correlation can be represented by $m = (250 \pm 30) - 320\beta$. Our $ZnCl_2$ with $\beta_{VV} = 0.71$ and $m \simeq 30$ data were included in ref 22. Alternatively, $ZnBr_2$ with $\beta_{VV} = 0.68 \pm 0.02$ and $m \simeq 45$ falls within this broad phenomenological correlation. Narrowing of $L(\log \tau)$ with decreasing fragility m was recently rationalized[30] by relating β and m with the fluctuation of the coordination number, reflecting the local structure of the liquid.

A second mechanism for nonexponential relaxation postulates the presence of different microdomains (spatial heterogeneity as the origin of the distribution of relaxation times).[10,11,31,32] In this case the distribution $L(\log \tau)$ results from the superposition of exponential correlation functions (eq 5) in different microenvironments within this approach. The supercooled state might be viewed as a "two-fluid" mixture consisting of "loose" and "tight" cages. The latter can be also envisaged as aperiodic crystal (rigid) microphases.[8b,11b,32] Since the lifetime of the rigid domains or tight cages is identified as the primary α-relaxation, the distribution $L(\log \tau)$ likely arises from the wide size distribution of these microdomains. All these theoretical

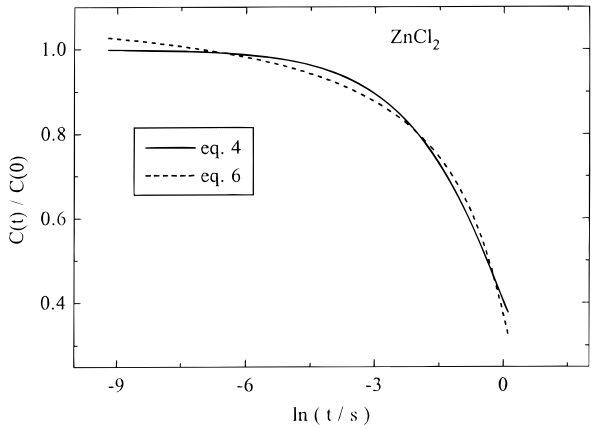

Figure 5. Comparison of the relaxation functions given in eq 4 with $\beta = 0.7$, $\tau^* = 1.25$ (solid line) and eq 6 (ref 31d) with $B = 4290$ K, $\tau_c = 2.2$ s, and $z_c = 9$ (dashed line). Equation 4 represents the experimental correlation function of $ZnCl_2$ at 403 K.

approaches involving spatial heterogeneities with different dynamics have in common the assumption of a second-order phase transition[33] from the supercooled to a solid phase, which is however dynamically inaccessible due to diverging energy barriers. Multidimensional NMR,[34] rotation of optical probes in a molecular glass former,[35] and Monte Carlo simulation data of facilitated kinetic Ising model[36] support the idea of spatially heterogeneous dynamics.

Besides the semiempirical eq 4, an analytical expression for the shape of the relaxation function relates $g(t)$ to the maximum size of the cooperatively rearranging microdomains:[31d]

$$g(t) \propto \exp[B/(Tz_c \ln(t/\tau_c))] \tag{6}$$

where the time τ_c is on the order of τ^* (eq 4) and $t < \tau_c$; z_c is the characteristic maximum number of structural units in these (polydisperse) microdomains, and B is the activation parameter in the common Vogel−Fulcher−Tammann (VFT) equation[1] describing the non-Arrhenius T-dependence of τ,

$$\tau = \tau_\infty \exp[B/(T - T_0)] \tag{7}$$

where T_0 denotes the ideal glass transition temperature. For $ZnCl_2$, $T_0 = 274$ K and $B = 4070$ K (see Figure 6, below). Parenthetically, application of eq 7 to describe the T-dependence of the α-relaxation times over a broad $t-T$ range has been criticaly examined recently.[12] In the present context, it is worth mentioning that eq 6 relates nonexponentiality to non-Arrhenius T-dependence, which is a pertinent feature in the strong versus fragile classification of glass formers.[1,22] To obtain an estimation of z_c, we have compared eq 4 with $\tau^* = 1.2$ s and $\beta = 0.70$, which describes the experimental $g(t)$ of $ZnCl_2$ at 403 K, with eq 6 using τ_c and z_c as adjustable parameters. A reasonable comparison between these two functions is obtained with $\tau_c = 2.2$ s and $z_c \simeq 9$ as visualized in Figure 5. From the value of z_c, a rough estimate of the largest size of the microdomains is about 20 Å.

Another picture related to the preceding models is a frustration-limited domain structure below a temperature T^* near and above the melting point.[3] This new thermodynamic model is distinguished by the absence of any liquid to solid phase transition below T_g, and hence T_g plays no role. The α-relaxation time is associated with the lifetime of the ordered microdomains whose size R_D is frustration limited below T^*. Their dissociation and formation proceeds via motion of the domain wall,[3,11] and the T-dependence of the characteristic τ below T^* is given by

$$T \log(\tau/\tau_0) = B^* T^* \epsilon^{8/3} \tag{8}$$

where $\epsilon \equiv (T^* - T)/T^*$ and $1/B^*$ is a measure of the frustration characteristic of the mesoscopic structure. τ_∞ and E_∞ are species-specific molecular parameters in the Arrhenius T-dependence $\tau_0 = \tau_\infty \exp(E_\infty/kT)$, which describes the expected T-dependence in the liquid state. The latter can be obtained from measurements at $T > T^*$, typically in the nanosecond (or faster) time range. Depolarized Rayleigh (DRS) and Brillouin scattering (BS) can measure relaxation in the GHz frequency range using Fabry−Perot interferometry. Reorientational (τ_2) and structural relaxation (τ) times in $ZnCl_2$ were obtained by DRS[20] and BS,[24] respectively.

Figure 6 shows the T-dependence of the experimental relaxation times τ obtained by PCS (eq 5), BS[24] for both $ZnCl_2$ and $ZnBr_2$, and ultrasonic[23] and DRS[20] for $ZnCl_2$. The plots of Figure 6 are based on the VFT eq 7 (inset) and on eq 8 with the solid lines denoting their fits to the experimental times. Here, we do not address the question which T-equation provides better representation.[12] Instead, we examine the physical meaning of the adjustable parameters with regard to the nature of the supercooled state. For the VFT eq 7 (dashed line in the inset of Figure 6), T_0 (=274 K), which is about 100 K lower than T_g, and the relatively high value of $B = 4070 \pm 50$ K reflect the intermediate behavior of $ZnCl_2$ in the strong versus fragile classification. For eq 8, the narrowly avoided transition T^* (=690 K) is about 20% higher than the melting temperature T_m (=593 K), and the value of the frustration parameter $1/B^*$ ($=9.4 \times 10^{-3}$) implies a rather small microdomain size R_D, as also inferred from the shape of the relaxation function (eq 6). The value of the high-T Arrhenius activation energy $E_\infty = 6400$ K (≈12.7 kcal/mol) reflects a network structure. For $ZnBr_2$, the parameters of eq 8 assume the values $E_\infty = 6390 \pm 50$ K, $1/B^* = (7.9 \pm 0.9) \times 10^{-3}$, and $T^* = 680 \pm 10$ K. As expected from the nature of T^*, it bears no relation to T_g, which is higher in $ZnBr_2$. It is worth mentioning that eq 7 gives a better representation of the PCS and DRS times (inset of Figure 6), whereas eq 8 provides better description of the PCS and BS times.

Unlike the situation in polymeric[7] and molecular fragile glass formers, the relaxation function $C_2(t)$ in these network-bonded inorganic glasses systematically exhibits a broader shape compared to $C_\rho(t)$, as reflected directly in $L(\log \tau)$ (Figure 4) and indirectly in the values of β (0.62 versus 0.72); $ZnBr_2$ appears to display a somewhat lower value of β for $C_\rho(t)$. Concurrently, the average relaxation times $\langle\tau\rangle = (\tau^*/\beta)\Gamma(1/\beta)$ ($\Gamma(1/\beta)$ being the gamma function) and the characteristic times at maximum $L(\log \tau)$ for the two relaxation functions are very close (Figure 4). In the aperiodic crystal picture[10b,11b,32] of glass-forming materials, α-relaxation relates to cooperative rearrangements on the boundaries of the immobilized solidlike regions and may therefore be responsible for both translational and orientational motion (eqs 2, 3); coupling of reorientation and translational motions was assumed[27] to derive an analytical expression of eq 3. Compatible with the observed coupling between the fluctuations in the local density and optical anisotropy are similar heterogeneous views of the supercooled state involving a frustration-limited domain structure[3] or "patchwork" of domains,[11,32] where structural relaxation is determined by the domain-wall areas. Recent molecular dynamics simulations[37] have also shown that the translational relaxation time compares well with τ_{or} for q less than about 1 $Å^{-1}$, which is fulfilled in the present low q's. At high q, translational relaxation is faster than reorientation.[37] The disparity however in the shapes of $C_2(t)$ and $C_\rho(t)$ is a pertinent

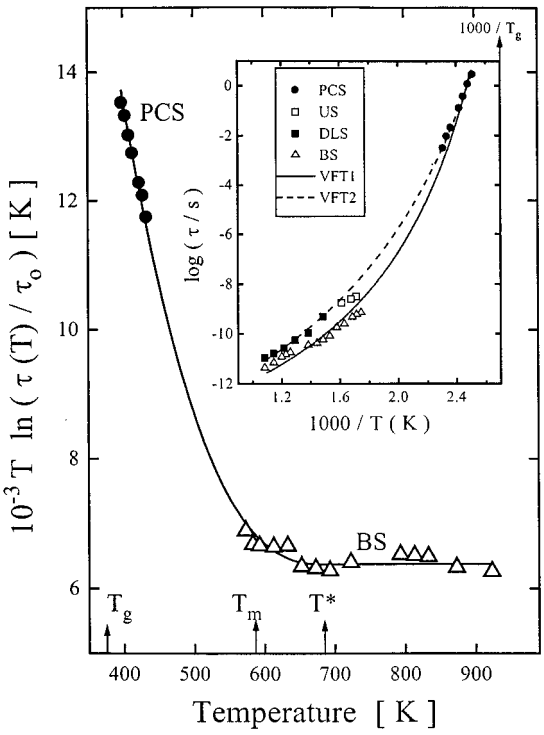

Figure 6. Temperature of the α-relaxation times for pure $ZnCl_2$ in the liquid and supercooled state as obtained from photon correlation spectroscopy (PCS), Brillouin scattering (BS, ref 24d), depolarized Rayleigh scattering (DRS, ref 20), and ultrasonic measurements (US, ref 23). The fit of eq 8 is indicated by the solid line, whereas the VFT (eq 7) representation is shown in the inset.

aspect which still awaits explanation. In view of eq 4 and the current picture of a supercooled state, this experimental finding might reflect slight differences in the barriers imposed to pure reorientations, compared to translational motions. The energy landscape should reflect the relative importance of attractive and repulsive parts of interactions,[4,32] and their modification in the mixture could affect the relaxation functions $C_2(t)$ and $C_\rho(t)$.

Symmetric Binary Mixture. Zinc chloride and zinc bromide form virtually ideal mixtures, as evidenced by the negligible small excess enthalpy of mixing.[38] On the basis of this locally homogeneous static structure, an equimolar $ZnCl_2-ZnBr_2$ mixture should display α-relaxational characteristics intermediate between those of the pure components. It is evident, however, from the distributions of relaxation times shown in Figure 4 that the relaxation functions $C_\rho(t)$ and $C_2(t)$ of the mixture measured at the same T now possess distinctly different shapes and relaxation times. Moreover, the slow process is significantly suppressed in the orientation correlation function (Figure 3) relative to the pure components.

The α-relaxation in the mixed glass (fast process in Figures 2 and 3) remains a single process, despite the presence of small but finite concentration fluctuations. Due to the cooperative nature of the α-relaxation, mapping of slow concentration fluctuations into a composition-dependent cooperative volume (ξ^3) could lead[16] to a two-step α-relaxation, if the two components have sufficiently large T_g contrast. The presence of two distinctly different local time scales has been reported for mixed polymer systems so far.[16] In this context, the unimodal distribution of relaxation times (Figure 3) is consistent with the small T_g contrast ($\Delta T_g = 15$ K) in the present mixture. Moreover, at length scales ξ (over which a coherent molecular motion occurs) the system should be homogeneous, implying a short correlation length for the concentration fluctuations. In

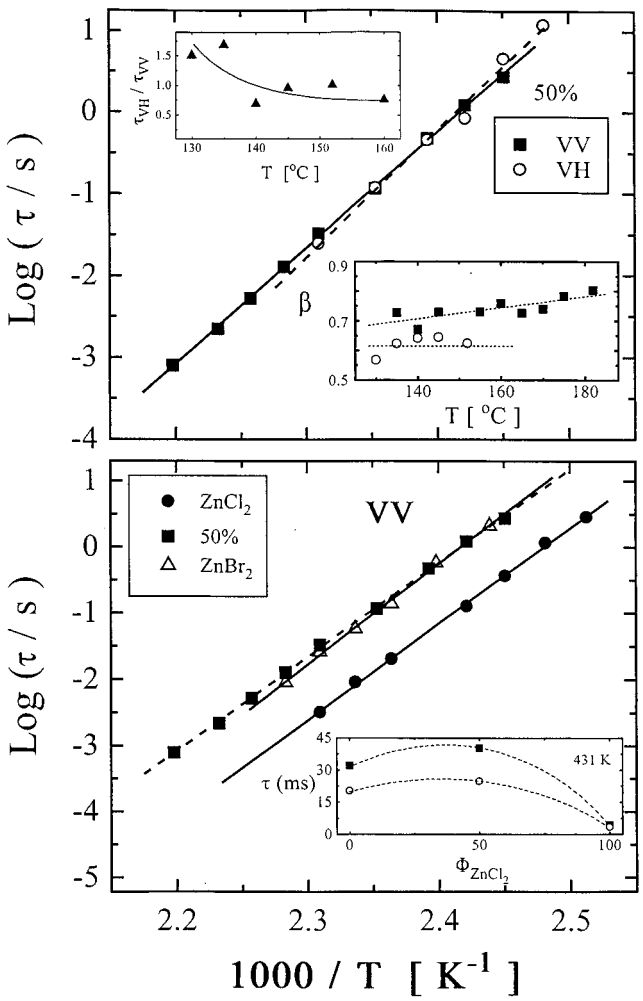

Figure 7. Arrhenius plot of the α-relaxation times in $ZnCl_2$, $ZnBr_2$, and their symmetric mixture obtained from PCS measurements near T_g. Upper part: Relaxation times of density (VV) and orientation (VH) fluctuations in the mixture. Inset: Temperature variation of the ratio $τ_{VH}/τ_{VV}$ and the shape parameter β. Lower part: Relaxation times of density fluctuations in the mixture and pure componets. Inset: Composition dependence of the relaxation times at 431 K.

view of the ideal mixing, the latter should be small, whereas ξ ($\propto z_c$ in eq 6) is about 20 Å. In the mixture, an independent estimate of ξ can be obtained from the comparison between the local α-relaxation time and the mutual diffusion time $\tau_c(q)$. From PCS measurements at 310 °C, $D = 1/(\tau_c q^2) = 2.3 \times 10^{-8}$ cm^2/s and $\tau \simeq 1 \times 10^{-8}$ s as estimated from the extrapolation (eq 7) at this high temperature. Hence, τ corresponds to the translational diffusion time over $\xi \approx 10$ Å; the lower value of ξ compared to the 20 Å above is compatible with the higher T.

The α-relaxation times obtained from the $C_\rho(t)$ and $C_2(t)$ correlation functions of the mixture are shown in the Arrhenius plot of Figure 7 (upper) along with the values of the shape parameters (inset of Figure 7 (upper)). The relaxation times for the $C_\rho(t)$ in the three samples are shown in Figure 7 (lower), where the composition dependence of the relaxation times for both $C_\rho(t)$ and $C_2(t)$ at constant T is visualized in the inset. The main findings emerging from Figures 3, 4, and 7 are (i) the disparity between the shape parameters of $C_2(t)$ and $C_\rho(t)$ and the narrowing of the shape for the latter with increasing T; (ii) the stronger variation of the orientational time τ_2 with T; and (iii) the closeness between the α-relaxation times of the mixture and the high-T_g component $ZnBr_2$.

The distribution of the α-relaxation times and the temperature dependence of τ are related via the parameter z (eq 6) or B^*,

T^* (eq 8), which reflect collective behavior. If universal behavior is emphasized by ignoring the effect of the local molecular properties, then different experimental probes (cf. eqs 2 and 3) employed to study glass dynamics should yield the same values for the shape and temperature activation parameters.[39] In this respect, the difference in the α-relaxation parameters as observed by isotropic and anisotropic light scattering is a remarkable result. In the current physical picture of the primary α-relaxation, this observation implies that the size of the cooperatively rearranging microdomains (eqs 6 and 8) should affect differently rotational and translational motion, depending probably on the fragility of the glass.[7,14] The existing models of liquid−glass transition do not address this issue,[39] which would require the link between microscopic molecular properties, e.g., E_∞, T_0 (eq 8), and mesoscopic collective properties, e.g., β, B^*, T^*.

It has been recently reported[8] that translational diffusion in fragile molecular[8a,b] and polymeric glasses[8c] as measured by optical grating techniques displays a weaker T-dependence than reorientation times which follow the T-dependence of the macroscopic shear viscosity. An increase in long-lived spatial heterogeneities as T is lowered toward T_g can rationalize[8c] this different T-dependence, since translational diffusion is mainly determined by mobile regions, whereas reorientation is heavily influenced by less mobile microregions. Assuming diffusive transport, it appears that the probe molecules translate several times their length within one reorientation time in the vicinity of T_g. However, on approaching T_g, translational motion was found to become nondiffusive.[8c] In this context, we recall that the correlation time τ measured here for $C_\rho(t)$ is insensitive to q variations in the region of low q's ($q < 0.05$ nm^{-1} in section III). By assuming the validity of Stokes−Einstein and Debye−Stokes−Einstein equations, respectively, for translational and rotational relaxation of a particle of size R, the root mean square (rms) displacement in one τ_2 is $\langle r^2 \rangle \approx R^2(\tau_2/\tau)$. Hence, the similarity between τ_2 and τ suggests that the rms displacement in one rotational correlation time is on the order of the particle size.

While the mixture is thermodynamically ideal, its α-relaxation time deviates from a linear interpolation between the values of the correlation times of the pure components and instead approaches the values of pure $ZnBr_2$ (Figure 7 (lower)). A representation of the temperature dependence in terms of eq 8 yields[24d] $T^* = 705$ K, $1/B^* = 9 \times 10^{-3}$, and $E_\infty = 6350$ K, which are indeed close to the corresponding values for pure $ZnBr_2$. Alternatively, the main difference with the α-relaxation times of $ZnCl_2$ relates to the value of T^*, which is 15 K higher in the symmetric mixture. Formally, in terms of eq 8, it is the value of the narrowly avoided transition T^* which should be similar in the mixture and $ZnBr_2$, whereas in terms of the free volume picture of eq 7, T_0 should assume a similar value in the two systems. A theoretical account for the dynamic asymmetry, i.e., domination of the slow component dynamics in the ideal symmetric mixture, is, however, missing.

Slow Process. The VV light scattering from fragile organic glass formers[10] displays an additional process, slower than the α-relaxation, with an exponential shape, a diffusive (q^2-dependent) rate, and pronounced intensity at low q's. This slow process could hardly be resolved in the VH light scattering and has been assigned to long-range density fluctuations,[10] probably due to the spatial distribution of the cooperatively rearranging microregions associated with the α-relaxation. The correlation functions of Figures 2 and 3 clearly show that this process is also present in the significantly less fragile zinc halide glasses. Whenever this slow process is the dominant feature of the $C_\rho(t)$, the amplitude α_ρ of the latter is lower[7,14] than α_2 for the $C_2(t)$, despite the relationship $I^*_{VV}(t) = I_\rho(t) + (4/3)I^*_{VH}(t)$; for the mixture (Figure 3), $\alpha_\rho = 0.35$ and $\alpha_2 = 0.6$.

On the basis of the experience so far, an unexpected result is the appearance of the slow process in the anisotropic scattering, as shown in Figures 2 and 3. The VH activity of the slow process near T_g has been verified for four different $ZnCl_2$ samples; far above T_g, there is no slow process in the VH scattering (Figure 2). As indicated by the intensity profiles (inset of Figures 2 and 3), the presence of the slow VH process in $ZnCl_2$ and $ZnBr_2$ is associated with enhanced average VH scattering intensity compared to the I_{VH} of the mixture and $ZnCl_2$ at 260 °C; the mixture exhibits a much weaker slow process in the VH scattering. The relaxation time and the intensity of the slow process were found to increase with decreasing q. However, a quantitative estimation of this dependence would require fully relaxed experimental correlation functions (Figures 2 and 3). The dynamics of the slow process in the present systems could be better studied at higher temperatures, if the onset of crystallization did not preclude studies in that T range.

Excess VH intensity could also arise from the presence of strains near T_g; however, these should relax much slower than the long-range density fluctuations of the VV slow mode. A second origin of the excess VH intensity might be fluctuation-induced second-order scattering, as recently observed in critical polymer blends[40] near the macrophase separation. In this case, the excess I_{VH} intensity is proportional to the square of the intensity of the slow VV process, whereas the relaxation rates of the two processes are not very different. However, the last speculation remains to be proven. Nevertheless, verification of the slow VH process in other glass-forming liquids and a detailed study of its characteristics might provide further insight into the glass transition dynamics.

V. Concluding Remarks

The density and orientation correlation functions in two noncrystalline zinc halides measured by PCS near T_g reveal single moderately broad relaxation time distributions and temperature dependences for the relaxation times which are characteristic of glasses with intermediate fragility. In the current physical picture of the dynamic structure of glasses, these results support microheterogeneities with length scales on the order of 2 nm. The correlation functions of dynamic variables, e.g., $\alpha_{yz}(q,t)$, $\rho(q,t)$ coupled to the same vitrification process can have different shapes apparently reflecting species-dependent molecular characteristics.

The two zinc halides form a thermodynamically ideal mixture, which however shows dynamic asymmetry. The α-relaxation of the 50% mixture resembles closely that of $ZnBr_2$, the component with the higher T_g. The additional slow process in the mixture affects mainly the polarized light scattering spectrum, like in fragile molecular and polymeric glass formers. In contrast, the slow process in the pure components is also present in the anisotropic scattering.

References and Notes

(1) (a) Mohanty, U.; Oppenhein, I.; Taubes, C. H. *Science* **1994**, *266*, 425. (b) Angell, C. A. *Science* **1995**, *267*, 1924. (c) Frick, B.; Richter, D. *Science* **1995**, *267*, 1939. (d) Sokolov, A. P. *Science* **1996**, *273*, 1675.

(2) Götze, W.; Sjögren, L. *Rep. Progr. Phys.* **1992**, *55*, 241.

(3) (a) Kivelson, S. A.; Zhao, X.; Kivelson, D.; Fischer, T. M.; Knobler, C. M. *J. Chem Phys.* **1994**, *101*, 2391. (b) Kivelson, D.; Kivelson, S. A.; Zhao, X.; Nussinov, Z.; Tarjus, G. *Physica A* **1995**, *219*, 27. (c) Kivelson, D.; Tarjus, G.; Zhao, X.; Kivelson, S. A. *Phys. Rev. E* **1996**, *53*, 751.

(4) Stillinger, F. H. *Science* **1995**, *267*, 1935.

(5) Fytas, G.; Meier, G. In *Dynamic Light Scatering. The Method and Some Applications*; Brown, W., Ed.; Oxford Science Publ.: Oxford, 1993; p 407.

(6) Du, W. M.; Li, G.; Cummins, H. Z.; Fuchs, M.; Toulouse, J.; Knauss, L. A. *Phys. Rev. E* **1994**, *49*, 2192.

(7) Reinhardt, L.; Fytas, G.; Fischer, E. W.; Willner, L. *Acta Polym.* **1996**, *47*, 399.

(8) (a) Fujara, F.; Geil, B.; Sillescu, H.; Fleischer, G. *Z. Phys.* **1992**, *B88*, 195. (b) Rössler, E.; Eiermann, P. *J. Chem. Phys.* **1994**, *100*, 5237. (c) Cicerone, M. T.; Blackburn, F. R.; Ediger, M. D. *Macromolecules* **1995**, *28*, 8224.

(9) At high q's the structural relaxation time becomes strongly q-dependent: Colmenero, J.; Alegria, A.; Arbe, A.; Frick, B. *Phys. Rev. Lett.* **1992**, *69*, 478.

(10) (a) Gerharz, B.; Meier, G.; Fischer, E. W. *J. Chem. Phys.* **1992**, *92*, 71110. (b) Fischer, E. W. *Physica* **1993**, *A201*, 183. (c) Zetsche, A.; Fischer, E. W. *Acta Polym.* **1994**, *45*, 168.

(11) (a) Bendler, J. T.; Schlesinger, M. F. *J. Phys. Chem.* **1992**, *96*, 3970. (b) Kirkpatrick, T. R.; Thirumalai, D.; Wolynes, P. G. *Phys. Rev.* **1989**, *A40*, 1045. (c) Stillinger, F. H. *J. Chem. Phys.* **1988**, *89*, 6461. Stillinger, F. H.; Hodgdon, I. A. *Phys. Rev.* **1994**, *E50*, 2064.

(12) (a) Stickel, F.; Fischer, E. W.; Richert, R. *J. Chem. Phys.* **1995**, *102*, 6251. (b) Cummins, H. Z. *Phys. Rev. E* **1996**, *54*, 5870. (c) Kivelson, D.; Tarjus, G.; Xiao, X. L.; Kivelson, S. A. *Phys. Rev. E* **1996**, *54*, 5873.

(13) Kivelson, D. *J. Chem. Phys.* **1991**, *95*, 709.

(14) Yannopoulos, S. N.; Papatheodorou, G. N.; Fytas, G. *Phys. Rev. E.* **1996**, *53*, R1328.

(15) Köhler, W.; Fytas, G.; Steffen, W.; Reinhards, L. *J. Chem. Phys.* **1996**, *104*, 208.

(16) (a) Kumar, S. K.; Colby, R. H.; Anastasiadis, S. H.; Fytas, G. *J. Chem. Phys.* **1996**, *105*, 3777. (b) Fytas, G., Meier, G.; Richter, D. *J. Chem. Phys.* **1996**, *105*, 1208.

(17) Lai, C. C.; Macedo, P. B.; Montrose, C. J. *J. Am. Ceram. Soc.* **1975**, *58*, 120.

(18) (a) Pavlatou, E. A.; Rizos, A. K.; Papatheodorou, G. N.; Fytas, G. *J. Chem. Phys.* **1991**, *94*, 224. (b) Sidebottom, D. L.; Sorensen, C. M. *J. Chem. Phys.* **1989**, *91*, 7153.

(19) (a) Bucaro, J. A.; Dardy, H. D.; Cosaro, R. D. *J. Appl. Phys.* **1975**, *46*, 741. (b) Sidebottom, D.; Bergman, R.; Börjesson, L.; Torell, L. M. *Phys. Rev. Lett.* **1993**, *71*, 2260.

(20) Lebon, M. J.; Dreyfus, L.; Li, G.; Aouadi, A.; Cummins, H. Z.; Pick, R. M. *Phys. Rev. E* **1995**, *51*, 4537.

(21) Allen, D. A.; Howe, R. A.; Wood, N. D.; Howells, W. S. *J. Chem. Phys.* **1991**, *94*, 5071, and references therein.

(22) Böhmer, R.; Ngai, K. L.; Angell, C. A.; Plazek, D. J. *J. Chem. Phys.* **1993**, *99*, 4221.

(23) (a) Gruber, G. J.; Litovitz, T. A. *J. Chem. Phys.* **1964**, *40*, 13. (b) Mackenzie, J. D.; Murphy, W. K. *J. Chem Phys.* **1960**, *33*, 366.

(24) (a) Gunilla Knappe, H. E. *J. Chem. Phys.* **1984**, *80*, 4788. (b) Soltwisch, M.; Sukmanowski, J.; Quitmann, D. *J. Chem. Phys.* **1987**, *86*, 3207. (c) Zhu, H. M.; Sato, Y.; Yamamura, T. Y.; Sugimoto, K. In *Proceedings of 8th International Symposium on Molten Salts*; Gale, R. J., Blomgren, G., Kojima, H., Eds.; The Electrochemical Society Inc.: Pennigton, NJ, 1992; Vol. 92-16, p 41. (d) Yannopoulos, S. N. Ph.D. Thesis, Univ. of Patras, 1996.

(25) (a) Maisano, G.; Majolino, D.; Mallamace, F.; Cacciola, M. L.; Vasi, C. *Solid State Commun.* **1986**, *57*, 509. (b) Magazu, S.; Maisano, G.; Mallamace, F.; Migiardo, P.; Aliotta, F.; Vasi, C. *Phil. Mag. B* **1987**, *56*, 155.

(26) Berne, B. J.; Pecora, R. *Dynamic Light Scattering*; Wiley: New York, 1976.

(27) (a) Wang, C. H.; Fischer, E. W. *J. Chem. Phys.* **1985**, *82*, 632. (b) Wang, C. H. *J. Chem. Phys.* **1992**, *97*, 508.

(28) Cummins, H. Z.; Li, C.; Du, W.; Pick, R. M.; Dreyfus, C. *Phys. Rev. E* **1996**, *53*, 896; **1997**, *55*, 1232.

(29) Ngai, K. L.; Rendell, R. W.; Plazek, D. J. *J. Chem. Phys.* **1994**, *94*, 3088.

(30) Vilgis, T. A. *Phys. Rev.* **1993**, *B47*, 2882.

(31) (a) Miles, D. O.; Hasamoto, A. S. *Nature* **1962**, *193*, 644. (b) Adams, G.; Gibbs, J. H. *J. Chem. Phys.* **1965**, *43*, 139. (c) Grest, G. S.; Cohen, M. H. *Adv. Chem. Phys.* **1981**, *48*, 455. (d) Matsuoka, S.; Quan, X. *Macromolecules* **1991**, *24*, 2770.

(32) Tanaka, H. *J. Chem. Phys.* **1996**, *105*, 9375.

(33) Sethna, J. P.; Shore, J. D.; Huang, M. *Phys. Rev.* **1991**, *B44*, 4943.

(34) Schmidt-Rohr, K.; Spiess, H. W. *Phys. Rev. Lett.* **1991**, *66*, 3020.

(35) Cicerone, M. T.; Blackborn, F. R.; Ediger, M. D. *J. Chem. Phys.* **1995**, *103*, 5684.

(36) Foley, M.; Harrowell, P. *J. Chem. Phys.* **1993**, *98*, 5069.

(37) Roe, R. J. *J. Chem. Phys.* **1994**, *100*, 1610.

(38) Papatheodorou, G. N.; Kleppa, O. J. *Z. Anorg. Chem.* **1973**, *401*, 132.

(39) Ngai, K. L.; Mashimo, S.; Fytas, G. *Macromolecules* **1988**, *21*, 3030.

(40) Fytas, G.; Vlassopoulos, D.; Meier, G.; Likhtmann, A.; Semenov, A. N. *Phys. Rev. Lett.* **1996**, *76*, 3586.